Quantum well intermixing for the fabrication of InGaAsN/GaAs lasers with pulsed anodic oxidation

Y. Qu, C. Y. Liu, and Shu Yuan[a)]
School of Materials Engineering, Nanyang Technological University, Singapore 639798

S. Z. Wang and S. F. Yoon
School of Electrical and Electronic Engineering, Nanyang Technological University, Singapore 639798

Michael C. Y. Chan
Department of Electrical and Electronic Engineering, The University of Hong Kong, Hong Kong, People's Republic of China

M. H. Hong
Data Storage Institute, Singapore 117608

Quantum well (QW) intermixing was carried out by post-growth rapid thermal annealing in InGaAsN/GaAs QW laser structures grown by solid-source molecular-beam epitaxy. The intensity and width of the photoluminescence peak showed a dependence on annealing temperature and time, and the maximum intensity and minimum linewidth were obtained after the wafer was annealed at 670 °C for 60 s. The peak luminescence energy blueshifted with increasing annealing time, although it plateaued at an annealing time that corresponded to that yielding the maximum luminescence intensity. The diffusion coefficient for indium was determined from a comparison between experimental data and modeling, but showed that QW intermixing alone was not sufficient to account for the relatively large blueshift after annealing. Defects related to the incorporation of nitrogen in the QW layer were responsible for the low photoluminescence efficiency in the as-grown samples and were annealed out during rapid thermal annealing. During annealing, nitrogen interstitials moved to vacancy sites within the QW and thus suppressed QW intermixing. After annealing wafers under conditions giving the maximum luminescence intensity, lasers were fabricated with pulsed anodic oxidation. © *2004 American Institute of Physics.*
[DOI: 10.1063/1.1651322]

I. INTRODUCTION

Semiconductor lasers emitting at a wavelength of 1.3 μm are highly desirable for fiber optic communications. Traditionally, such lasers are made of InGaAsP-based materials grown on InP wafers. Such lasers, however, are expensive and have poor high-temperature characteristics. Vertical cavity surface emitting lasers (VCSELs) are ideal for data communications at 1.3 μm; however, it is very difficult to fabricate VCSELs on InP substrates, due to the low refractive index contrast between InP-based materials. The InGaAsN/GaAs material system grown on GaAs substrate, however, offers a potential solution to these problems.[1–4] The addition of N to InGaAs/GaAs system reduces the compressive strain in the InGaAs layer, lowers the interband transition energies of InGaAs/GaAs quantum wells (QWs) and increases the conduction band offset, resulting in a longer emission wavelength (suitable for making 1.3 μm lasers) and promising better high-temperature characteristics for 1.3 μm laser diodes.[5]

Unfortunately, InGaAsN/GaAs lasers suffer from low luminescence efficiency due to nonradiative centers caused by the incorporation of N.[6] Post-growth annealing reduces this problem significantly,[7] although the exact mechanism by which this is achieved is still debated.[8–10] Spruytte *et al.*[9] argued that defects associated with excess nitrogen in the material were responsible for the low luminescence efficiency, while Pan *et al.*[7] proposed that interdiffusion of In-Ga and N-As was responsible for the improvement of material quality by using rapid thermal annealing (RTA) at low temperature ($\sim$650 °C) and high temperature ($\sim$900 °C), respectively. In comparison, Tournie *et al.*[11] proposed that low growth temperature was responsible for the low radiative efficiency. In this work, we report a systematic study on QW intermixing (QWI) using RTA in InGaAsN/GaAs laser structures and obtain optimum RTA conditions for our laser structures in terms of luminescence intensity and peak width. We also include results from a laser fabricated using the optimum RTA conditions. Pulsed anodic oxidation[12–14] is a simple method for the fabrication of semiconductor lasers. We have recently achieved a significant reduction of threshold current density in AlGaInP lasers by using this method.[15] Pulsed anodic oxidation was used to form current blocking layers for the ridge waveguide InGaAsN lasers.

II. EXPERIMENT

The laser structures were grown by rf nitrogen plasma-assisted solid-source molecular-beam epitaxy (MBE). The

---

[a)]Electronic mail: assyuan@ntu.edu.sg

TABLE I. Laser wafer structure used in this work. The QWI wafer used in the QW intermixing study had the same structure, except that the upper cladding layer was not grown.

Layer	Thickness (nm)	Doping (1/cm^3)	Growth temperature (°C)
GaAs	200	Be 1×10^{19}	580
Al$_{0.4}$Ga$_{0.6}$As	1500	Be 5×10^{17}	610
GaAs	150	Undoped	580
In$_{0.32}$Ga$_{0.68}$As$_{0.983}$N$_{0.017}$	7	Undoped QW	460
GaAs	40	Undoped	580
In$_{0.32}$Ga$_{0.68}$As$_{0.983}$N$_{0.017}$	7	Undoped QW	460
GaAs	40	Undoped	580
In$_{0.32}$Ga$_{0.68}$As$_{0.983}$N$_{0.017}$	7	Undoped QW	460
GaAs	150	Undoped	580
Al$_{0.4}$Ga$_{0.6}$As	1500	Si, 5×10^{17}	610
GaAs	500	Si, 1×10^{18}	580
(100) GaAs substrate	400 μm	Si, 1×10^{18}	

growth chamber was equipped with standard effusion cell for arsenic and phosphorus, and the active nitrogen species were supplied by rf nitrogen plasma source. The samples were grown on (001) n-GaAs substrates that were Si-doped to a carrier concentration of $\sim 1 \times 10^{18}$ cm^{-3}. Prior to the growth, surface oxide desorption was carried out under As flux at a beam equivalent pressure (BEP) of 6.2×10^{-6} T. (2×4) surface reconstruction was maintained throughout the entire growth process. The BEPs for Ga and As were 4.5×10^{-7} and 6.2×10^{-6} T, respectively. The As/Ga flux ratio was fixed at 14. The growth rate was ~ 1.0 μm/h, verified by time-resolved reflection high-energy electron diffraction measurements. The nitrogen plasma source worked optimally at a nitrogen background pressure of 1.0×10^{-5} T and at an arsenic BEP$_{As}$ of 6.2×10^{-6} T, and was activated by a rf power greater than 60 W to maintain the plasma in high brightness mode. Si and Be were used for n-type and p-type doping of the epitaxial layers, respectively. Two wafers were grown under the same conditions, one of which was used for the fabrication of the laser (termed "laser wafer"), the other for studying QWI (termed "QWI wafer"). The QWI wafer had the same structure as the laser wafer, except that the upper p-type cladding layer was not grown. The layer structures for these samples are listed in Table I. After the growth, the wafer was diced into small pieces of 3 mm×3 mm. A thin (~ 200 nm) SiO$_2$ protection film was deposited on the samples prior to the annealing by electron-beam evaporation.

The samples were placed in the center area of a 4-in. Si wafer which was then loaded into the RTA chamber. The RTA chamber was purged with argon gas at 5 l/min for 5 min before the temperature was ramped up at a rate of 50 °C/s. After that, the gas flow was fixed at 2 l/min throughout the rest of the process. At high temperature, the temperature uniformity was within ±5 °C across the whole 4-in. wafer. After RTA, photoluminescence (PL) measurements were performed at 77 K using an Ar ion laser beam (the 514.5 nm line), a spectrometer, and a thermal-electronically cooled InGaAs detector connected to a lock-in amplifier.

After RTA and PL measurements, the annealing conditions to maximize the luminescence intensity and minimize

the width of the luminescence peak were identified and used in the fabrication of InGaAsN/GaAs/AlGaAs lasers. 50 μm photoresist stripes were first made by standard photolithography, and the mesas were then etched in a solution of phosphoric acid, hydrogen peroxide, and deionized water. With the photoresist still on the ridges, pulsed anodization was performed to form the current blocking layer. The voltage pulse duration was 1 ms, and the period was 12 ms, and total anodization time was 6 min. The wafer was thinned to ~ 100 μm thick and Au/Zn/Au and Au-Ge/Ni layers were deposited by electron-beam evaporation on the p-type and n-type sides, respectively, and annealed to make the ohmic contacts. Approximately 1200-μm cavity length laser bars were then cleaved and individual lasers were sawed. The uncoated lasers were tested on a probe stage with junction side up.

III. MODELING OF QWI

In this work, the effects of RTA were experimentally characterized using PL measurements. The blueshift (i.e., shift towards higher photon energies) in PL peak energy results from the changes in the band structure after RTA.[16] Pan *et al.*[7] proposed that at relatively low annealing temperatures (~ 650 °C), In-Ga interdiffusion dominates, and at higher temperatures (~ 900 °C) N-As interdiffusion becomes important. In this work, the maximum RTA temperature was 680 °C, so only In-Ga interdiffusion was taken into account in the modeling. Due to In and Ga interdiffusion, the QW shape changes from square to a smoothed one, which is usually described by the error function. This changes the electron and hole subband energies, and therefore changes (blueshifts) the PL energy. Therefore, a calculation of the interband transition energy that takes into account the change in strain in the QW and the changes in carrier confinement profiles due to Ga and In interdiffusion will yield the diffusion coefficients and will shed light on the complex interdiffusion processes.

The extent of the interdiffusion process is generally characterized by a diffusion length L_d, defined here as $L_d = \sqrt{Dt}$, where D is the interdiffusion coefficient for indium and t is the annealing time. We assumed an isotropic interdiffusion of In and Ga with the diffusion coefficients being independent of their respective concentrations, which were also assumed to be equal and constant; that is, Fick's second law of diffusion applies. The diffused In composition profile $w(z)$ across the QW structure is given by

$$w(z) = \frac{w_o}{2}\left[\operatorname{erf}\left(\frac{L_z + 2z}{4L_d}\right) + \operatorname{erf}\left(\frac{L_z - 2z}{4L_d}\right) \right], \qquad (1)$$

where w_o is the as-grown In mole fraction in the well, L_z is the as-grown width of the QW, and z is the coordinate along the growth direction (QW is centered at $z = 0$). Further details of the modeling are described elsewhere.[17–21]

The calculated QW interband transition energies were fitted to the measured PL peak energies by adjusting the value of D, thus D was determined.
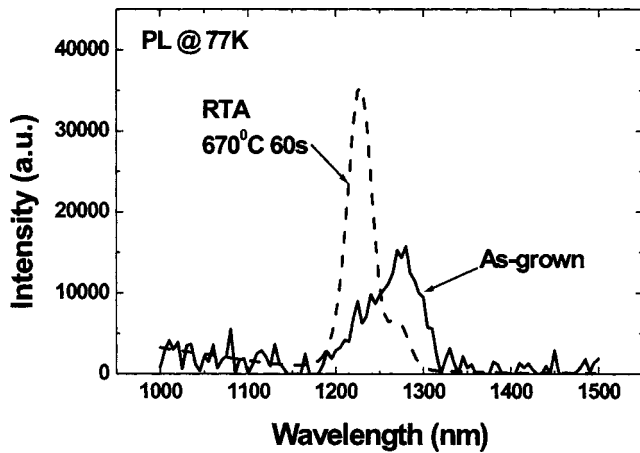
FIG. 1. Typical PL spectra from as-grown QWI wafer and QWI wafer annealed at 670 °C for 60 s.

FIG. 3. PL linewidth (FWHM) from the QWI wafer as a function of annealing time for different RTA temperatures.

IV. PL MEASUREMENTS

To study the effects of RTA on the QW intermixing in InGaAsN/GaAs samples and to find the optimum conditions for luminescent efficiency, we measured PL spectra at 77 K for as-grown and annealed samples. Figure 1 shows typical spectra for a piece of QWI wafer (as-grown) and a piece of QWI wafer annealed at 670 °C for 60 s. After annealing, the PL intensity increased significantly, and the linewidth also narrowed, indicating an increase in the radiation efficiency. It has been proposed that the incorporation of nitrogen into InGaAs layer introduces nonradiative centers (crystal defects or impurities).[9] Annealing reduced the nonradiative center density. The photon energy was also shifted to shorter wavelength.

Figure 2 shows the PL intensity from the QWI wafer as a function of annealing time for four different RTA temperatures between 630 and 680 °C. The PL intensity was taken as the integrated area under the peak. The overall trend is that optimized intensity can be found under conditions between 650 and 680 °C for around 60 s. Pan *et al.*[7] annealed their M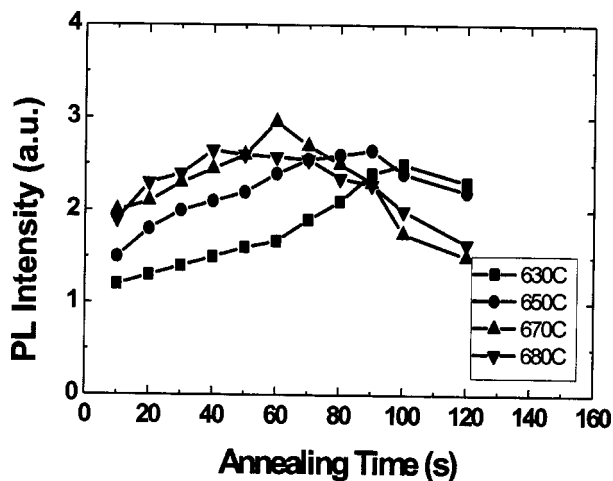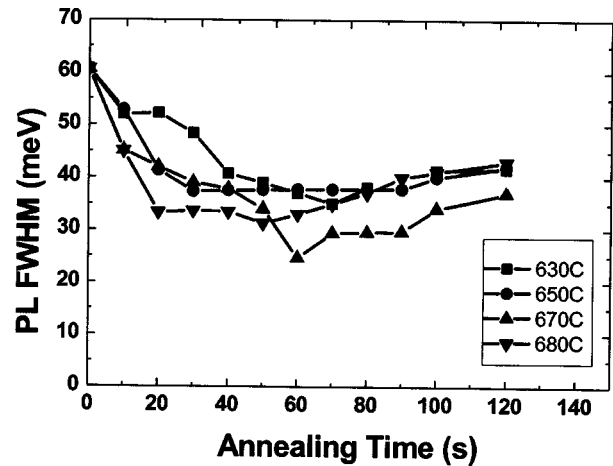BE-grown InGaAsN/GaAs QWs at 650 °C for durations up to 30 min (much longer than our 60 s), and observed that RTA generally improved the PL intensity, with intensity increasing with annealing time. They also found that for InGaAs/GaAs QW samples the PL intensity was insensitive to RTA annealing. They annealed samples at 900 °C, and found that PL intensity reached the maximum after 5 s annealing, and then dropped with annealing time for both InGaAs/GaAs and InGaAsN/GaAs samples. Kageyama *et al.*[10] annealed InGaAsN/GaAs QWs grown by chemical-beam epitaxy at a fixed duration of 30 s and found that maximum PL intensity was obtained at 675 °C. While Kageyama's InGaAsN QW had only 0.7% N, noticeably lower than 1.7% N in our laser structure, and their samples were grown not by MBE, nevertheless, their optimum temperature was essentially the same as ours, and their optimum RTA duration was shorter than demonstrated in this study (30 s versus 60 s). Xin *et al.*,[5] however, found that the maximum PL intensity was achieved with an anneal temperature of about 850 °C for InGaAsN/GaAs QWs, much higher than our optimum temperature of about 670 °C.

PL linewidth as measured by full width at half-maximum (FWHM) is also an important parameter for studying the luminescence efficiency. Figure 3 shows FWHM as a function of RTA time for different temperatures. For all annealing temperatures, it reaches a minimum for a duration of around 60 s. The smallest peak width of 25 meV was measured after annealing at 670 °C for 60 s, conditions which also yielded the highest PL intensity as shown in Fig. 2.

The PL photon energy also shifted towards higher energies with annealing time, as shown in Fig. 4. For all the temperatures, the blueshift was larger than 20 meV even when annealing for as little as 10 s. Yuan *et al.*[12] recently reported RTA annealing of InGaAs/GaAs QW samples at 825 °C for 30 s and observed negligible blueshift. The relatively large blueshift in this work might be due to (1) the effect of the SiO₂ encapsulation, which was deposited onto the sample before RTA, and (2) the incorporation of nitrogen into InGaAs layers. SiO₂ is well know to enhance QW intermixing in InGaAs/GaAs[22] and GaAs/AlGaAs[23] QWs be-

FIG. 2. PL intensity from the QWI wafer as a function of annealing time for different RTA temperatures.
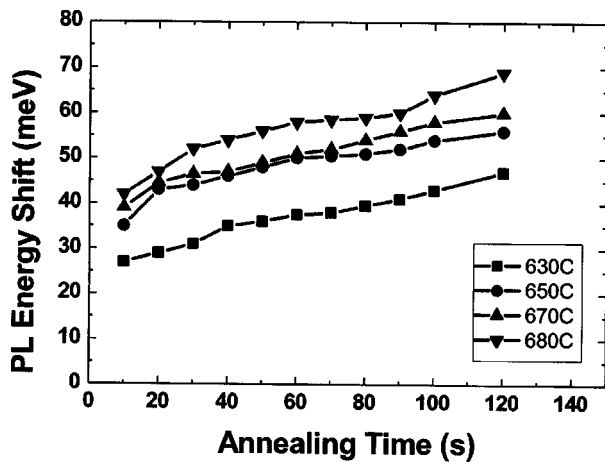
FIG. 4. PL photon energy shift with respect to the peak photon energy of the as-grown sample as a function of annealing time for different RTA temperatures.

FIG. 5. Diffusion length versus annealing time for QWI wafer samples annealed at 670 °C.

cause of the large diffusion coefficient of Ga in SiO_2, which increases Ga vacancies in GaAs and in turn enhances Ga and In interdiffusion. Similar effects have also been observed in GaNAs/GaAs QWs.[24] Burker *et al.*[22] did RTA in InGaAs/GaAs QWs capped with SiO_2 at temperatures higher than 850 °C. From their results, we estimate a diffusion coefficient value of about $5 \times 10^{-17} cm^2/s$ at 700 °C for 15 s. In this work, a diffusion coefficient value of $3.4 \times 10^{-16} cm^2/s$ for the annealing at 680 °C for 20 s has been determined, which is much higher than the above estimation from Ref. 22. Thus, the SiO_2 cap alone does not account for the large blueshift observed in this work.

It is possible that the incorporation of nitrogen into InGaAs/GaAs QW also enhances the interdiffusion of In and Ga atoms. Since QW intermixing is usually enhanced by an increase in the number of group-III vacancies, it is possible that the incorporation of nitrogen into InGaAs QW layer generated group-III vacancies (in addition to producing nitrogen interstitials). The blueshift increased with RTA time from 0 to about 50 s, then remained constant at around 60 s, and after about 80 s, it started to increase again. The blueshift is an indication of atom interdiffusion (e.g., In and Ga interdiffusion) in the QW, which is often enhanced by increasing group-III vacancy density.[21] The plateauing of the blueshift at around 60 s in Fig. 4 coincides with the maximum PL intensity in Fig. 2, indicating a minimization in vacancy density by RTA under those conditions. Spruytte *et al.*[9] found that as-grown samples contained a significant concentration of interstitial nitrogen that disappeared following a 1 min anneal at 760 °C. It is well known that if the vacancies in the sample are occupied by other atoms the number of vacancies is reduced and atomic interdiffusion can be suppressed. For example, in Ref. 25, Zn diffused from *p*-type GaAs substrate into GaAs/AlGaAs QWs, occupying vacancy sites within the QW, suppressing the Ga-Al atomic interdiffusion, and reducing the blueshift in the PL spectra.[25] If interstitial nitrogen atoms in our samples had moved to occupy some of the vacancies during the annealing, especially under the "optimum" RTA conditions (i.e., 670 °C for 60 s), the QW intermixing could be suppressed, resulting in
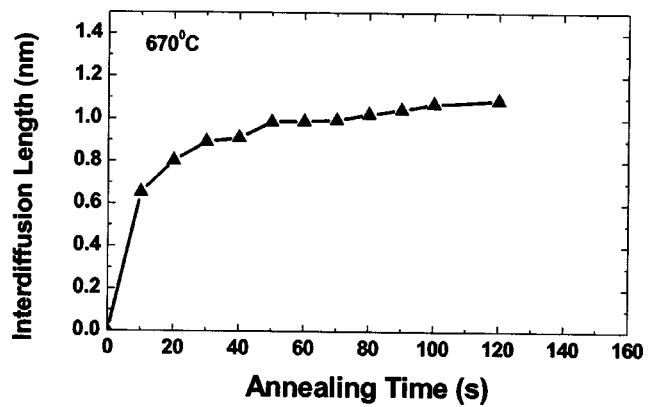
the plateauing of the PL blueshift, as shown in Fig. 4. It is possible that the reduction in the number of vacancies and nitrogen interstitials reduced the scattering of photon-generated carries in the PL measurement, leading to the reduction of the PL line width shown in Fig. 3.

The diffusion length was determined as outlined in Sec. III, and is shown as a function of RTA time in Fig. 5 for RTA temperature of 670 °C.

V. InGaAsN/GaAs LASERS FABRICATED WITH PULSED ANODIC OXIDATION

The laser wafer was annealed at 670 °C for 60 s (the annealing conditions that yielded the maximum PL intensity), then processed into lasers using the pulsed anodic oxidation method. The lasers were tested in cw mode at 18 K, and the optical and electrical characteristics are shown in Fig. 6. Lasing was observed at currents above 250 mA. The laser from this material shows a total slope efficiency at $T = 18$ K of 16 mW/50 mA$=0.32$ W/A. As a comparison, values around 0.48 W/A were routinely obtained from InGaAsP laser at room temperature.[26] Due to the relatively poor quality of the wafer, no lasers were fabricated from wafers that
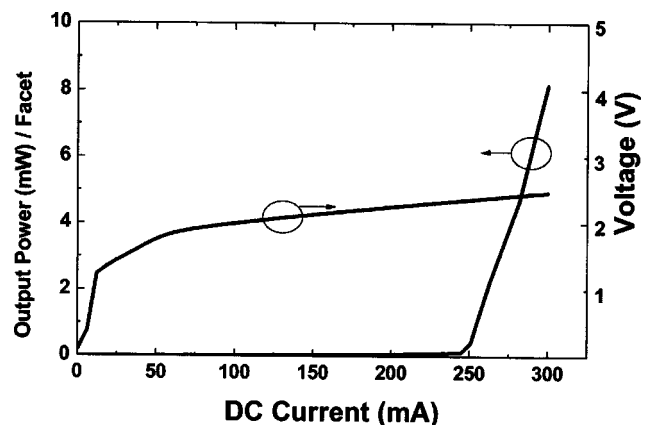
FIG. 6. Light output power of per facet versus current ($L-I$) and voltage versus current ($V-I$) characteristics at 18 K for a 50 μm$\times$1200 μm laser diode that was annealed at 670 °C for 60 s and fabricated with pulsed anodic oxidation.
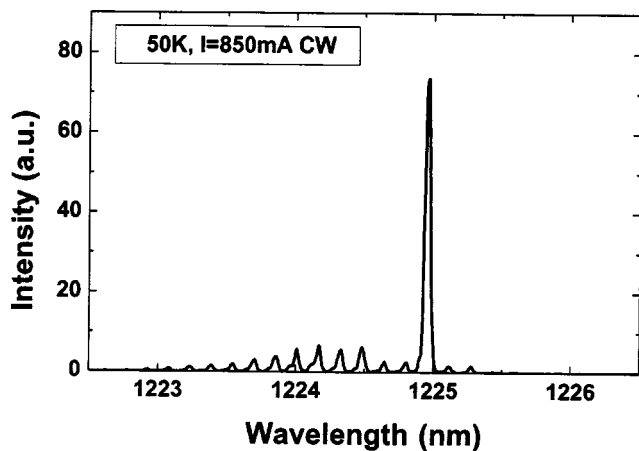
FIG. 7. Emission spectrum at 50 K for the same laser diode characterized in Fig. 6.

were annealed under other conditions. Work is in progress to grow higher quality wafers. Figure 7 shows a typical laser emission spectrum at 50 K.

VI. CONCLUSIONS

In this work, two InGaAsN/GaAs structures were grown by solid-source MBE. One was a laser structure, and the other was the same except that the upper cladding layer was not grown. RTA was carried out at temperatures from 630 to 680 °C and QW intermixing-was observed. Maximum PL intensity and minimum linewidth at half-maximum were obtained after annealing at 670 °C for 60 s. The PL photon energy blueshifted annealing time, but it plateaued under the annealing conditions, yielding the maximum luminescence intensity. Determining the diffusion coefficient from a comparison between experimental data and modeling showed that QW intermixing alone was not sufficient to account for the relatively large blueshift measured after annealing. Defects related to the incorporation of nitrogen in the QW layer were responsible for the low PL efficiency in as-grown samples and were annealed out during RTA. During the annealing, nitrogen interstitials moved to take up some vacancy sites in the QW and thus suppressed QW intermixing. Lasers were fabricated with pulsed anodic oxidation after annealing under optimized conditions.

ACKNOWLEDGMENTS

[1] W. Ha, V. Gambin, M. Wistey, S. Bank, S. Kim, and J. S. Harris, Jr., IEEE Photonics Technol. Lett. **14**, 591 (2002).
[2] N. Tansu, A. Quandt, M. Kanskar, W. Mulhearn, and L. J. Mawst, Appl. Phys. Lett. **83**, 18 (2003).
[3] C. S. Peng, T. Jouhti, P. Laukkanen, E. M. Pavelescu, J. Konttinen, W. Li, and M. Pessa, IEEE Photonics Technol. Lett. **14**, 275 (2002).
[4] O. Malis, W. K. Liu, C. Gmachl, J. M. Fastenau, A. Joel, P. Gong, S. W. Bland, and N. Moshegov, J. Cryst. Growth **251**, 432 (2003).
[5] H. P. Xin, K. L. Kavanagh, M. Kondow, and C. W. Tu, J. Cryst. Growth **201/202**, 419 (1999).
[6] T. K. Ng, S. F. Yoon, S. Z. Wang, W. K. Loke, and W. J. Fan, J. Vac. Sci. Technol. B **20**, 964 (2002).
[7] Z. Pan, L. H. Li, W. Zhang, Y. W. Lin, R. H. Wu, and W. Ge, Appl. Phys. Lett. **77**, 1280 (2000).
[8] S. Z. Wang, S. F. Yoon, W. K. Loke, C. Y. Liu, and S. Yuan, J. Cryst. Growth **255**, 258(2003).
[9] S. G. Spruytte, C. W. Coldren, J. S. Harris, Jr., W. Wampler, P. Krispin, K. Ploog, and M. C. Larson, J. Appl. Phys. **89**, 4401 (2001).
[10] T. Kageyama, T. Miyamoto, S. Makino, F. Koyama, and K. Iga, Jpn. J. Appl. Phys. **38**, L298 (1999).
[11] E. Tournie, M. A. Pinault, and A. Guzman, Appl. Phys. Lett. **80**, 4148 (2002).
[12] S. Yuan, C. Y. Liu, F. Zhao, M. C. Y. Chan, W. K. Tsui, L. V. Dao, and X. Q. Liu, J. Appl. Phys. **93**, 9823 (2003).
[13] S. Yuan, C. Jagadish, Y. Kim, Y. Chang, H. H. Tan, R. M. Cohen, M. Petravic, L. V. Dao, M. Gal, M. C. Y. Chan, E. H. Li, and P. S. Zory, IEEE J. Sel. Top. Quantum Electron. **4**, 629 (1998).
[14] M. J. Grove, D. A. Hudson, P. S. Zory, R. J. Dalby, C. M. Harding, and A. Rosenberg, J. Appl. Phys. **76**, 587 (1994).
[15] C. Y. Liu, Shu Yuan, J. R. Dong, S. J. Chua, M. C. Y. Chan, and S. Z. Wang, J. Appl. Phys. **94**, 2962 (2003).
[16] S. Yuan, Y. Kim, C. Jagadish, P. T. Burke, M. Gal, J. Zou, D. Q. Cai, D. J. H. Cockayne, and R. M. Cohen, Appl. Phys. Lett. **70**, 1269 (1997).
[17] M. C. Y. Chan, C. Surya, and P. K. A. Wai, J. Appl. Phys. **90**, 197 (2001).
[18] D. Ahn and S. L. Chuang, IEEE J. Quantum Electron. **24**, 2400 (1988).
[19] S. L. Chuang, Phys. Rev. B **43**, 9649 (1991).
[20] D. J. BenDaniel and C. B. Duke, Phys. Rev. **152**, 683 (1966).
[21] S. Yuan, Y. Kim, C. Jagadish, P. T. Burke, M. Gal, M. C. Y. Chan, E. H. Li, and R. M. Cohen, J. Appl. Phys. **83**, 1305 (1998).
[22] S. Burkner, M. Baeumler, J. Wagner, E. C. Larkins, W. Rothemund, and J. D. Ralston, J. Appl. Phys. **79**, 6818 (1996).
[23] B. S. Ooi, S. G. Ayling, A. C. Bryce, and J. H. Marsh, IEEE Photonics Technol. Lett. **7**, 944 (1995).
[24] L. H. Li, Z. Pan, Y. Q. Xu, Y. Du, Y. W. Lin, and R. H. Wu, Appl. Phys. Lett. **78**, 2488 (2001).
[25] F. Zhao, I. W. Choi, S. Yuan, C. Y. Liu, J. Jiang, and M. Chan, Thin Solid Films **426**, 186 (2003).
[26] D. A. Ackerman, G. E. Shtengel, M. S. Hybertsn, P. A. Morton, R. F. Kazarinov, T. Tanbun-Ek, and R. A. Logan, IEEE J. Sel. Top. Quantum Electron. **1**, 250 (1995).